

## Article

# Effect of the Relative Positions of Di-Laterally Substituted Schiff Base Derivatives: Phase Transition and Computational Investigations

Fowzia S. Alamro <sup>1</sup>, Hoda A. Ahmed <sup>2,3,\*</sup> , Saheed A. Popoola <sup>4</sup> , Hamud A. Altaleb <sup>4</sup> , Khulood A. Abu Al-Ola <sup>5</sup> and Sobhi M. Gomha <sup>2,4,\*</sup>

<sup>1</sup> Department of Chemistry, College of Science, Princess Nourah Bint Abdulrahman University, Riyadh 11671, Saudi Arabia; fsalamro@pnu.edu.sa

<sup>2</sup> Department of Chemistry, Faculty of Science, Cairo University, Cairo 12613, Egypt

<sup>3</sup> Chemistry Department, College of Sciences, Taibah University, Yanbu 30799, Saudi Arabia

<sup>4</sup> Chemistry Department, Faculty of Science, Islamic University of Madinah, Al-Madinah Al-Munawwarah 42351, Saudi Arabia; abiodun@iu.edu.sa (S.A.P.); haltaleb@iu.edu.sa (H.A.A.)

<sup>5</sup> Chemistry Department, College of Sciences, Madina Monawara, Taibah University, Al-Madina 30002, Saudi Arabia; kabualola@taibahu.edu.sa

\* Correspondence: ahoda@sci.cu.edu.eg (H.A.A.); smgomha@gmail.com (S.M.G.)

**Abstract:** Two new laterally di-substituted derivatives namely, (E)-4-((2-Chlorophenyl)imino)methyl)-3-methoxyphenyl 4-(alkoxy)benzoate, were designed and investigated for their mesomorphic properties. Elucidation of their molecular structures was carried out by elemental analyses, NMR and FT-IR, spectroscopy. Phase transitions were examined by differential scanning calorimetry (DSC) and polarized optical microscopy (POM). The optimized geometrical architectures of both compounds were deduced theoretically using GAUSSIAN 09 program. In order to establish the most probable conformation for each compound, four probable conformations were predicted for their positional isomers which vary according to the orientations of the two lateral groups. The results were used to correlate the experimental measurements with the predicted conformations. The study revealed that the investigated derivatives are non-mesomorphic and the orientations, as well as positions of the two-lateral groups, have a significant effect on the molecular packing of the molecules, their geometrical and thermal parameters.

**Keywords:** Schiff base/ester; di-lateral groups; phase transition; computational calculations; DFT



**Citation:** Alamro, F.S.; Ahmed, H.A.; Popoola, S.A.; Altaleb, H.A.; Abu Al-Ola, K.A.; Gomha, S.M. Effect of the Relative Positions of Di-Laterally Substituted Schiff Base Derivatives: Phase Transition and Computational Investigations. *Crystals* **2021**, *11*, 870. <https://doi.org/10.3390/cryst11080870>

Academic Editors: Assem Barakat and Alexander S. Novikov

Received: 27 June 2021

Accepted: 24 July 2021

Published: 27 July 2021

**Publisher's Note:** MDPI stays neutral with regard to jurisdictional claims in published maps and institutional affiliations.



**Copyright:** © 2021 by the authors. Licensee MDPI, Basel, Switzerland. This article is an open access article distributed under the terms and conditions of the Creative Commons Attribution (CC BY) license (<https://creativecommons.org/licenses/by/4.0/>).

## 1. Introduction

The molecular geometries relationship between mesogenic cores of compounds and their mesomorphic behaviors are very important to understand. A number of Schiff base/ester homologous sets of thermotropic liquid crystal (LC) derivatives have been investigated and are often evaluated from the point of their interesting optical and computational characterizations [1–4]. From the geometrical investigations, we found that the linkage spacer orientation in the rigid core, the location of linking groups, lateral substitutions, the aspect ratio of the molecule, and the length of the attached terminal chain are essential parameters for mesophase behavior [5–12].

Today, the optoelectronic properties of materials are shown to be strongly enhanced by the introduction of lateral polar groups [13]. This enhancement is mainly dependent on the spatial orientation and location of the lateral substituent. The combination of more lateral groups enables the polar substituents to play an essential role in influencing the geometrical, thermal, and physical properties of the resultant LC compound, such as melting temperature, phase transition phenomena, morphology, polarizability, and dipole moment [14–17]. In addition, the lateral and terminal polar groups induce a significant impact on the mesomorphic properties of the imine/ester derivatives. The lateral group increases the intermolecular separation that broadens the core part and leads to a decrement

in the lateral interactions [18–20]. So, any increment in the molecular breadth will reduce the thermal stability of both the nematic and smectic phases [21].

The size of the lateral group is an important factor, of which the introduction of small size type into mesomorphic geometries causes no steric molecular disruption while the LC mesophases could still be observed. Moreover, the lateral substituent in the mesogenic core can disrupt the closed packing of molecules and reduce LC melting transition, thereby improving the solubility of LC effectively. In addition, the melting temperature of mesomorphic materials could be decreased to near room temperature by mixing two or more components. However, the phase transitions and thermal properties of LCs mixtures differ from their individual components. Thus, series of binary LC mixtures could be better made for certain applications [22]. This practice makes the mesomorphic behavior of such mixtures essential as it proffers the way to achieving lower melting points [23–25].

The polar lateral substituent changes the polarizability and the dipole-moment of the whole molecule to a ratio depending on its location and orientation. This definitely reflects on the mesomorphic behavior of the formed molecule. Moreover, as the length of the terminals increases, the molecules tend to orientate in a parallel arrangement [26]. The steric effects of di-lateral fluorine atoms on the mesomorphic properties of four ring compounds had been reported [27]. The study revealed that the derivatives exhibited high stable SmC and N mesophases with a wide mesophase range. Furthermore, the kind and thermal stability of the mesophase were reported to be dependent on the length of the terminal alkoxy-chain as well as the position of the di-fluoro substituents. Interestingly, the computational measurements have become an important approach in designing new compounds as it reveals series of information ranging from thermal and geometrical properties to molecular orbital energies as well as the molecular geometries of the LC materials [28–30].

The aim of the present study is to prepare a new di-laterally substituted Schiff base/ester liquid crystal system, **In**, exhibiting two asymmetrical terminals. The first terminal is an alkoxy chain connected to the phenyl benzoate moiety (Figure 1). The second wing is the lateral Cl attached to the phenylimine component. The central ring has a lateral methoxy group incorporated in the ortho position with respect to the imine linkage. We intend to justify our experimental results theoretically using the density functional theory (DFT) approach and explain the effect of insertion of two lateral substituents in the mesogenic cores of the molecule. Moreover, binary phase diagrams will be briefly discussed between mono and di-laterally systems.

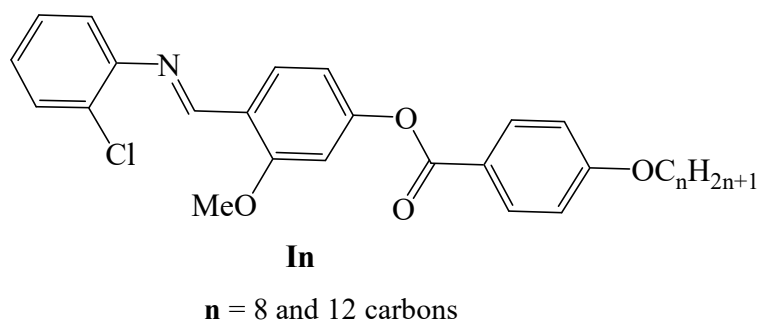
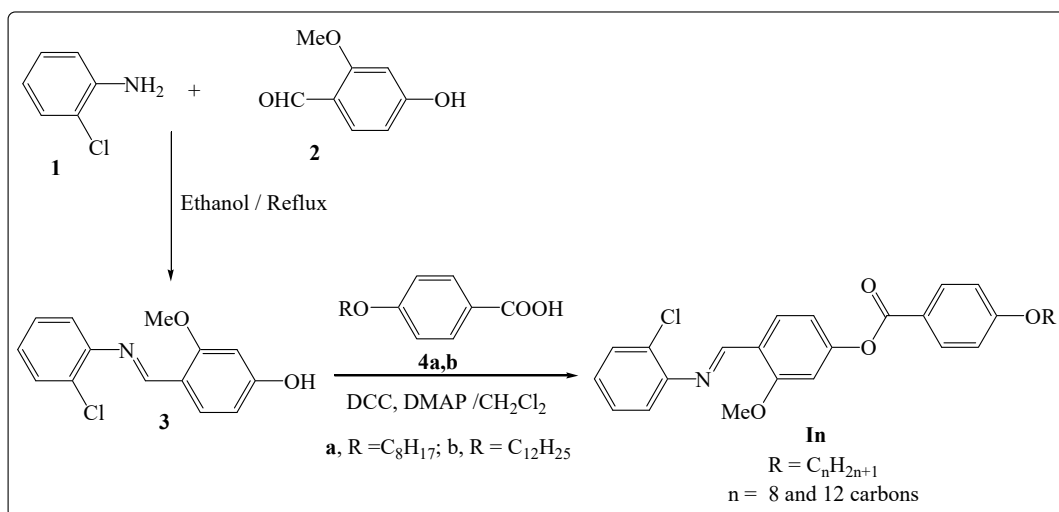


**Figure 1.** Molecular structures of investigated derivatives, **In**.

## 2. Experimental

### Synthesis

Hydrazones and Schiff bases are valuable intermediates in the synthesis of many heterocyclic systems that are used in various applications [31–40]. A series of new laterally di-substituted Schiff base derivatives **3** and **In** were formed as shown in Scheme 1.



**Scheme 1.** Synthesis route of the title compound, **In**.

Methods of preparations and the spectroscopic details of products **I8** and **I12** are highlighted in Supplementary Data.

The isomerization of present Schiff base di-laterally compounds (**In**, Figure 2a) and laterally neat derivatives (**IIn**, Figure 2b) have been investigated, the NMR spectra showed the presence of only one isomer for each and this is affirmed by the singlet-proton resonances of most of the aromatic protons of the designed compounds. Thus, the insertion of lateral Cl and -OCH<sub>3</sub> groups in ortho positions with respect to the imine-linkage may be stabilizing the Z-isomer rather than E-isomer (Figure 2a). This is further corroborated in the theoretical part.

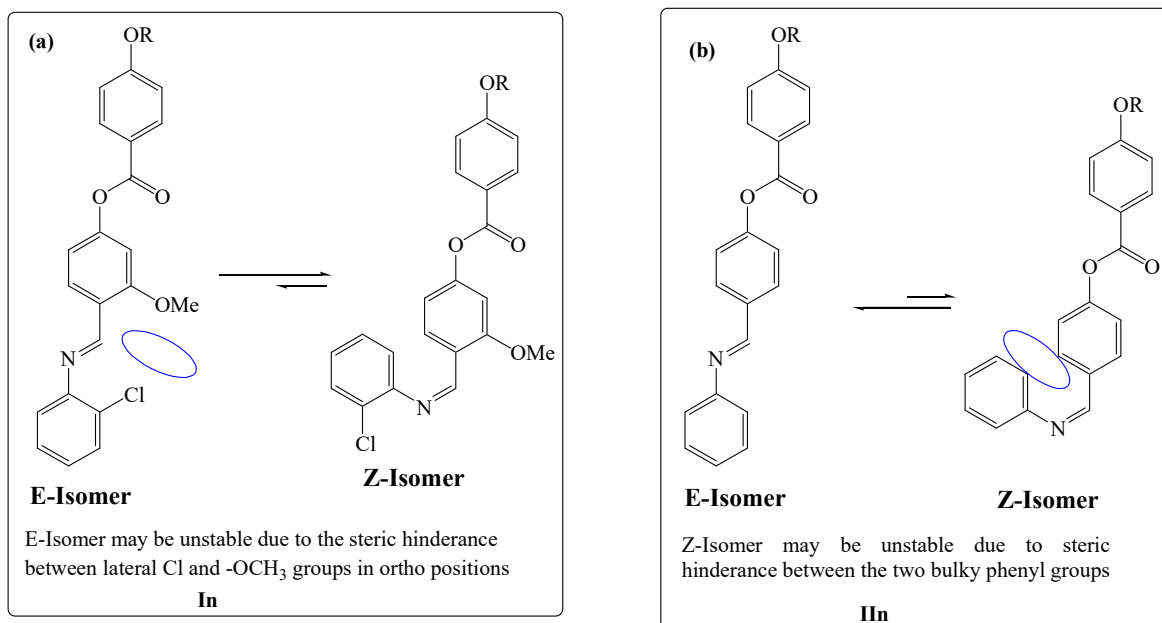


**Figure 2.** E- and Z- geometrical isomers of compounds, (a) **In** and (b) **IIn**.

### 3. Results and Discussion

#### 3.1. Mesophase and Optical Studies

The optical and mesomorphic behaviors for the designed di-laterally substituted derivatives, **In**, were evaluated by DSC while the mesophase type was checked using POM. Figure 3 shows the DSC thermograms of prepared compounds **I8** and **I12** through

heating and cooling scans. It is clearly shown in the Figure 3, only one endotherm characteristic peak of the Cr-to-I transitions was shown upon heating and reversed during the cooling cycle. The POM investigations revealed no texture of any mesophase thereby affirming the materials not to exhibit any mesomorphic properties either enantiotropically or monotropically. Moreover, the transition temperatures together with their associated enthalpy measured by DSC are listed in Table 1. The data revealed that the two prepared di-laterally substituted materials are non-mesomorphic accompanied with high values of enthalpy changes from solid to isotropic liquid. Since there are many factors affecting the formation of liquid crystal phases and these factors are being shared with different ratios to define the mesophase behavior [41–44]. First of them is the lateral adhesion of molecules that increases with the increment in either terminal-chain length or the aspect ratio. The terminal alkoxy chain length usually plays a key role in the stabilization of phases. The second important factor is the geometrical structure of the molecule, which in many cases is influenced by the steric hindrance of the attached lateral groups. Another one is the end-end interactions which depend mainly on the polarity and the length of the terminal wings and are attributed to the changes of polarizability. The linking spacers highly impact the conjugation within the mesogenic portion of the investigated molecule. In addition, the conjugated molecular structures of **In** derivatives (Figure 4) suggest that the insertion of one more double bond stabilized the molecules and increased the lateral dipole moments as well as the polarizability of the whole structure. It seems that the increase in length of molecule contributes to these effects. The different mesomeric interactions between the di-lateral groups and the imino linkage, which largely depend on their positions resulted in enhancement in the lateral dipole moments that consequently disrupted the phase transition phenomena.

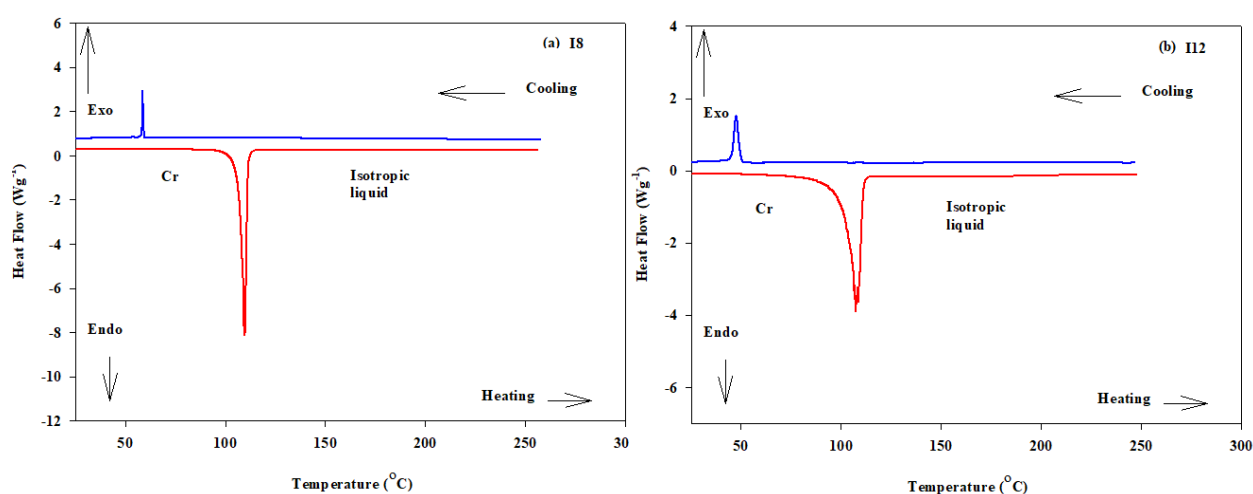


**Figure 3.** Thermograms driven from DSC for (a) sample **I8** and (b) sample **I12** at heating rate of  $10\text{ }^{\circ}\text{C min}^{-1}$ .

**Table 1.** Transition temperatures ( $^{\circ}\text{C}$ ) and their enthalpies  $\Delta H$ ,  $\text{kJmol}^{-1}$ , for compound, **In**.

Comp.	Upon Heating		Upon Cooling	
	$T_{\text{Cr-I}}$	$\Delta H_{\text{Cr-I}}$	$T_{\text{I-Cr}}$	$\Delta H_{\text{I-Cr}}$
<b>I8</b>	109.8	73.5	64.4	39.6
<b>I12</b>	107.3	52.72	55.9	35.4

Cr-I: transition from solid–isotropic liquid phase; I-Cr: transition from isotropic liquid–solid phase.

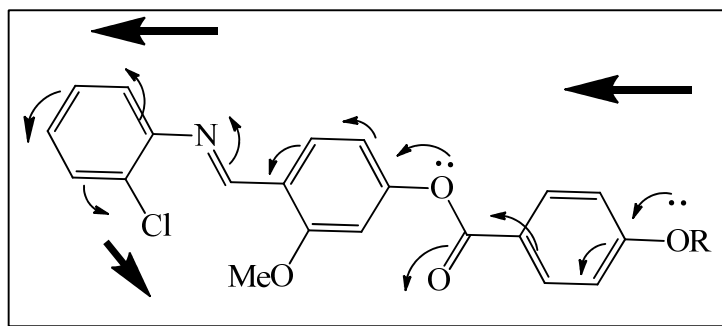
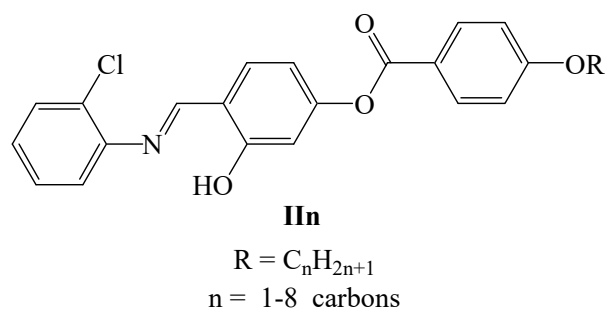


**Figure 4.** Conjugation of molecules, **In**.

It is worth noting that the increase in the length of the alkoxy group brings about a decrease in the molecular aggregation resulting from the terminal alkoxy chain oxygen, the strong -COO- moiety end-to-end intermolecular interactions, and the side-side cohesive forces between molecules. These interactions participate with different ratios and directly affect the formation of mesophase [45]. A competitive effect usually results from both types of interactions and this is affected by the change in the molecular conformation. Moreover, the steric effect of the two lateral groups could disrupt the molecular arrangements of molecules and eventually lead to non-mesomorphic behavior.

In another report, *N*-[4-(4-*n*-alkoxybenzoyloxy)-2-hydroxybenzylidene]-chloroanilines, **IIIn** (Scheme 2), were mesomorphically investigated via Raman spectroscopic measurements [46]. The compounds were found to exhibit nematic-phase. Their behaviors were influenced by the molecular conformations with changeable twist angles of the mesogenic part of the molecules. The difference in conformation affected the vibrational modes associated with the azomethine linkage, especially the CH out-of-plane vibration of the phenyl ring.



**Scheme 2.** Homologues series, **IIIn**.

### 3.2. Effect of the Insertion of Di-Lateral Substituents on the Mesophase Properties of Laterally-Neat Molecules

In order to investigate the effect of insertion of the di-lateral groups within the mesogenic part of the conformation, on the mesophase behavior of non-lateral derivatives [47] (**IIIIn**, Figure 5), the thermal properties of the present system (**In**) were compared with the previous laterally-neat system, **IIIIn** [47]. Both compounds of homologous series **IIIIn** are dimorphic having smectic A (SmA) and nematic (N) mesophases with high thermal stability. The comparison revealed that the formation of mesophase influenced the dipole-moment of the molecular mesogenic core which is mainly dependent on the number, type, and location of the attached polar groups. So, the addition of the lateral Cl and MeO groups disrupted the mesomorphic molecular packing and led to non-mesomorphic molecules.

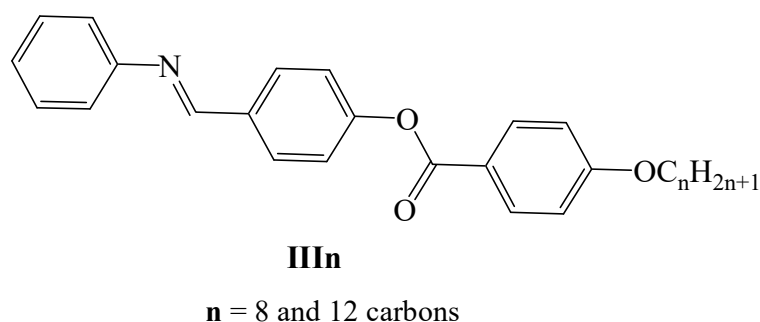


**Figure 5.** Molecular structures of **III<sub>n</sub>** series.

### 3.3. Calculated Geometrical Structures

The geometry of a material is an inherent property that dictates other properties showcased by the compound. Based on this, a potential energy scan (PES) was conducted on **I8** to establish the most stable geometry for the C=O of the –COO moiety, and the result is presented in Figure 6. All the density functional theory (DFT) estimations were conducted using the B3LYP method [41–43] with the basic set of 6-31g(d,p). Two stable configurations were predicted with the *cis* conformer (Figure S1) being more stable than the *trans* (Figure S1) counterpart by 0.1 kcal/mol. With respect to the direction of the two-lateral groups (–OCH<sub>3</sub> and –Cl), four possible conformations were predicted as depicted in Figure 7 while their relative energies are listed in Table 2. Conformer A with –OCH<sub>3</sub> in upward but –Cl in a downward direction with respect to the C=O was predicted to be most stable whereas the conformer D with both lateral groups in downward direction was found to be least stable. The higher stability of conformer A could be attributed to the least steric hindrance as compared to the others [48]. Having established the most stable conformation for the **I8**, the structure for the **I12** derivative was developed from it. The theoretical study revealed that the di-lateral groups at the ortho position with respect to the imine linkage have significant effects on the planarity and geometrical parameters of the molecule.

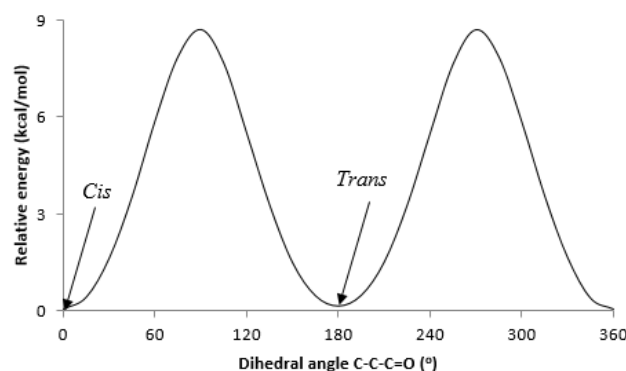


**Figure 6.** Potential energy scan of **I8** derivative.

**Table 2.** Relative stability of possible configurations for **I8** derivative.

Conformer	Relative Energy (kcal/mol)
A	0
B	0.57
C	1.60
D	2.03

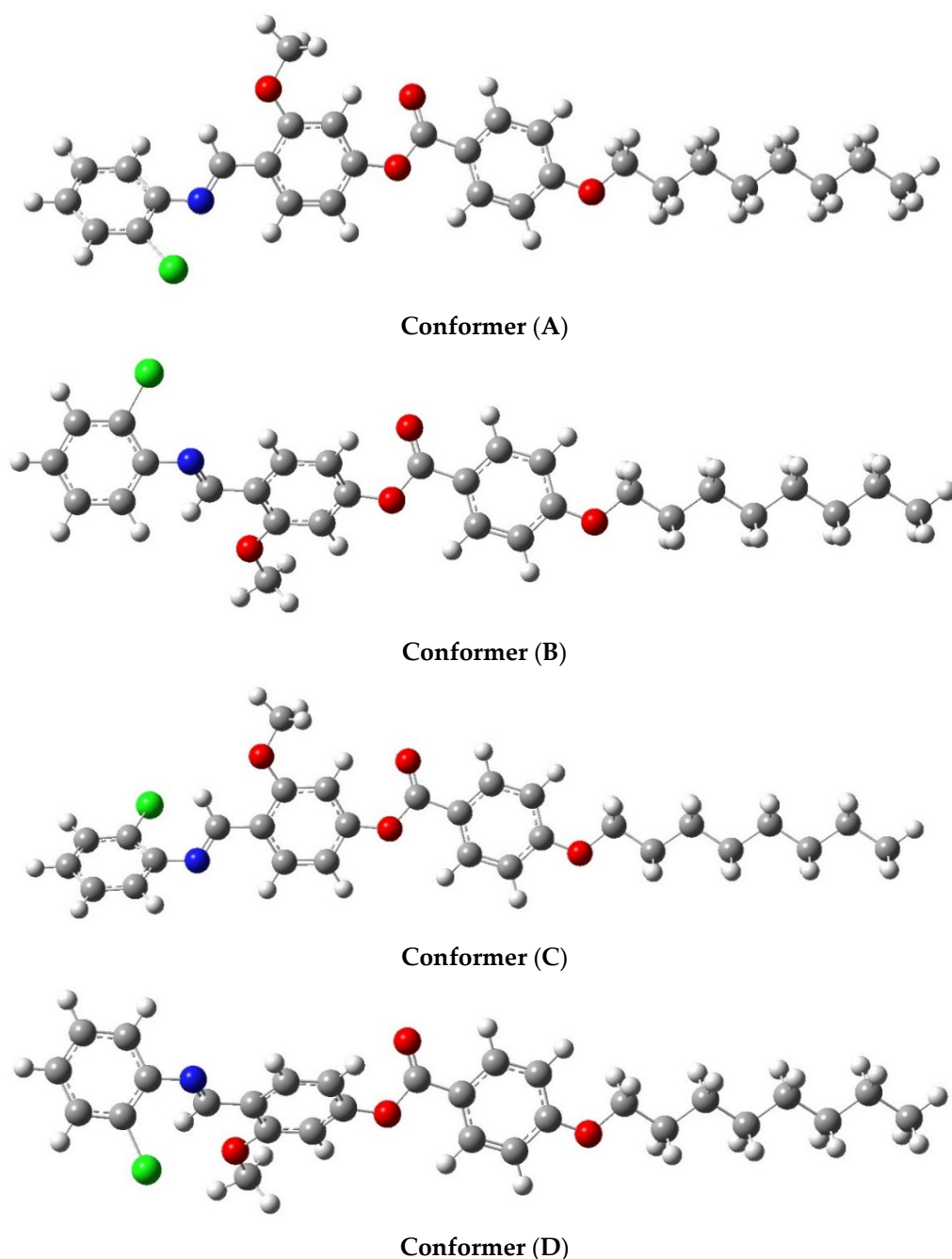


**Figure 7.** Possible configurations (A–D) for I8 derivative.

### 3.4. Reactivity Parameters

The parameters that showcase the reactivity of compounds (**In**) are the energy gap ( $\Delta E$ ) between HOMO and LUMO levels, ionization potential (I.P), and electron affinity (EA) [49]. However, the reactivity indicators listed in Table 3 affirm similar chemical reactivity for the I8 and the I12 as the same value was predicted for each of the corresponding parameters. Similar results were also obtained for their parent compounds. This shows that the reactivity of the derivatives is less sensitive to the increasing length of the terminal alkoxy chain. However, the effect of substitution could be noticed in the HOMO and LUMO energy levels and consequently on their HOMO–LUMO energy gap. The HOMO energies of I8 and I12 were pushed up while those of LUMO were reduced by the substitution. Furthermore, the resultant HOMO–LUMO energy gaps of the derivatives suggest better reactivity than their corresponding parent on the basis of a lower energy gap. On the part

of the dipole moment (Table 3), the derivatives were predicted to be more polar than their parents while the **I12** showed greater polarity over the **I8** counterpart. The higher polarity of **I12** is further corroborated by its higher dipole moment vectors obtained in all directions as depicted in Figure S2. On the other hand, the frontier molecular orbital presented in Figure 8 for both compounds (**I8** and **I12**) shows similar HOMO and LUMO distributions. For the HOMO, the electron clouds were evenly distributed over the carbon atoms and the  $\pi$ -electron of the two phenyl rings bearing the two-lateral groups as well as the  $-Cl$  substituent while the third phenyl ring and its alkoxy chain were highly electron deficient. However, for the LUMO, the distribution of electron clouds extended to the third phenyl ring bearing the alkoxy chain. Regarding the molecular electrostatic potential (MEP) shown in Figure 9, the shadowing of carbonyl oxygen and the lateral chlorine substituent by red cloud suggests a low electrostatic potential but high electron density for these regions. On the other hand, the blue cloud over the first alkoxy methylene and the neighboring phenyl hydrogen indicates low electron density but high electrostatic potential. In the same vein, an appreciable high electrostatic potential could be noticed for the methyl of lateral  $-OCH_3$  substituent. Moreover, as the chain length increases from  $n = 8$  to  $n = 12$  the polarizability of the molecule increases. This observation could be explained in the term of the ordering (packing) of molecules.

**Table 3.** Reactivity parameters, dipole moment, and polarizability of compound, **In**, calculated at the B3LYP/6-31g (d,p) level.

Compound	$E_{HOMO}$ , eV	$E_{LUMO}$ , eV	$\Delta E$ , eV	Dipole Moment, Debye	I.P, eV	E.A, eV	Polarizability, Bohr**3
Parent <b>I8</b>	−5.7884	−1.5706	4.2178	4.7234	5.7884	1.5706	361.0800
<b>I8</b>	−5.6638	−1.6376	4.0262	6.2805	5.6638	1.6376	394.3400
Parent <b>I12</b>	−5.7870	−1.5704	4.2167	4.7650	5.7870	1.5704	407.2600
<b>I12</b>	−5.6632	−1.6370	4.0262	6.3210	5.6632	1.6370	440.4900

### 3.5. Energy

Energy is an extensive property that depends on the size of a system. This assertion is affirmed by the calculated zero-point energy, thermal energy, and thermodynamic parameters highlighted in Table 4, as higher values were predicted for the **I12** with a bigger size than the **I8** counterpart. A similar trend was also found for their parents.

**Table 4.** Zero-point energy, thermal energy, and the thermodynamic parameters calculated at B3LYP/6-31g (d,p).

Compound	ZPE	Thermal	Enthalpy	Gibbs	Entropy
Parent <b>I8</b>	332.6148	351.9779	352.5703	289.1309	212.7770
<b>I8</b>	347.3236	369.0807	369.6730	301.0824	230.0540
Parent <b>I12</b>	404.0518	426.8706	427.4629	355.0759	242.7870
<b>I12</b>	418.9163	444.0788	444.6718	367.5357	258.7160

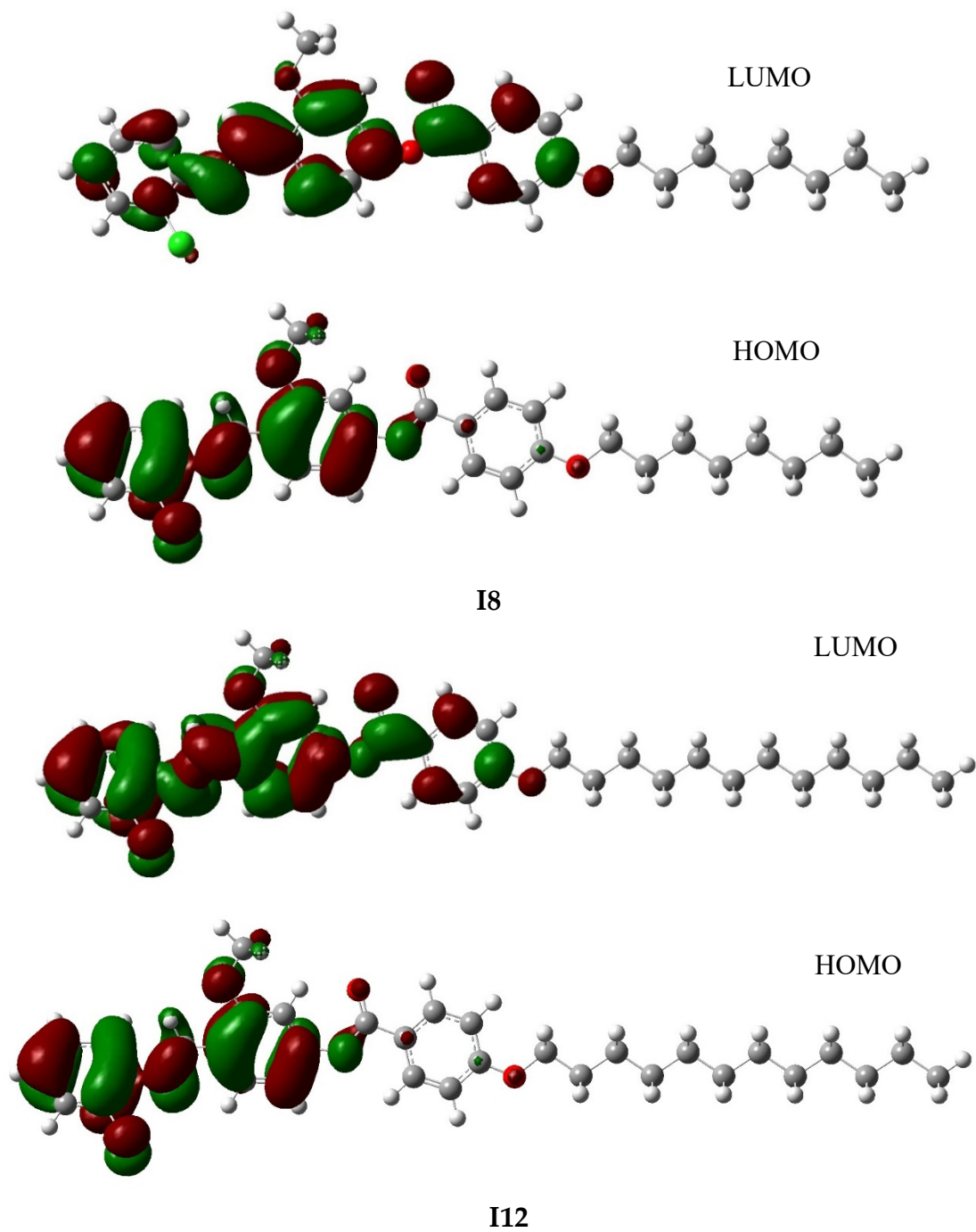
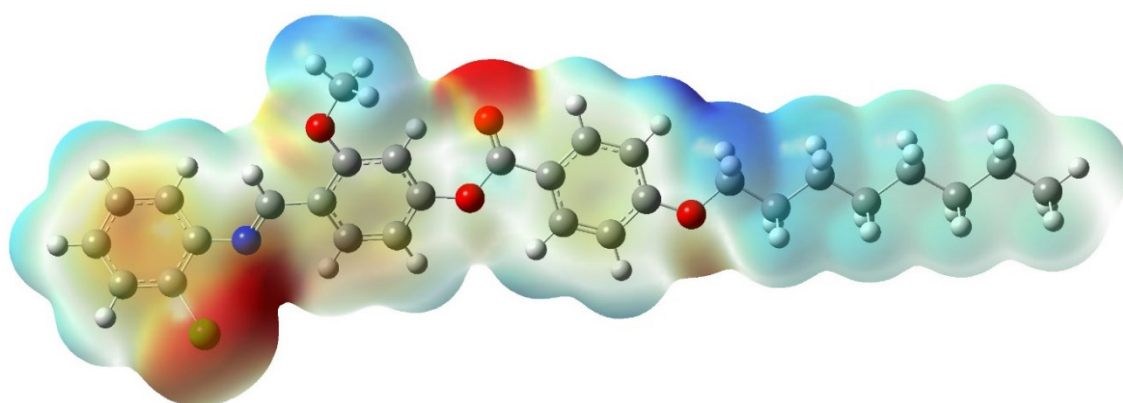
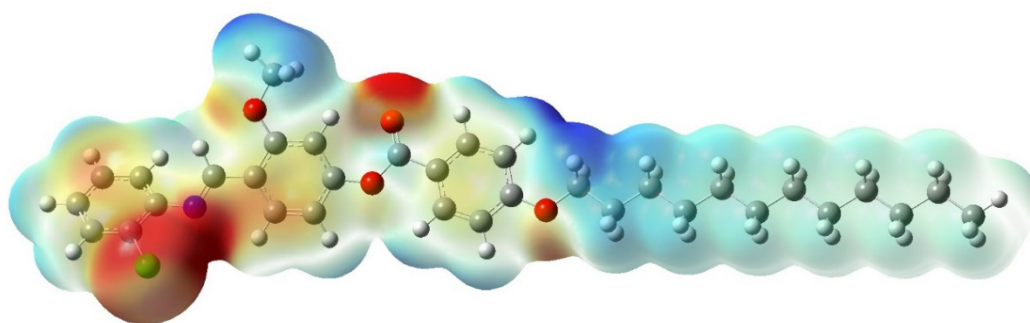


Figure 8. Frontier molecular orbital calculated at B3LYP/6-31g (d,p) for the I8 and I12 derivatives.



I8



I12

**Figure 9.** MEP calculated at B3LYP/6-31g(d,p) for the I8 and I12 derivatives.

#### 4. Conclusions

New asymmetric di-laterally substituted liquid crystal derivatives, (E)-4-(((2-Chlorophenyl) imino)methyl)-3-methoxyphenyl 4-(alkoxy)benzoate were designed and mesomorphically investigated. The lateral Cl and MeO groups introduced into the terminal and central rings respectively, influenced the lateral dipole moment and disrupted the molecular symmetry, and consequently resulted in non-mesomorphic materials. Four conformations were predicted for the homolog I8 by the DFT calculations. The deduced conformations were found to vary according to the relative location and orientation of the two lateral groups (Cl and MeO) attached to the terminal and central benzene rings. Moreover, a good agreement was found between the predicted conformations and the experimental data. Results revealed that the different mesomeric interactions between the di-lateral groups and the imino linkage, which largely depends on their positions, influenced the lateral dipole moments, geometrical parameters and consequently disrupted the phase transition properties of the molecules.

**Supplementary Materials:** The following are available online at <https://www.mdpi.com/article/10.3390/cryst11080870/s1>, Figure S1: The geometry of C=O established from the potential energy of C-C-C=O dihedral angle of I8 derivative. Figure S2. Atomic charges and dipole moment vectors, calculated at B3LYP/6-31G(d,p) level for the I8 and I12 derivatives. Figure S3. <sup>1</sup>H-NMR spectra of compound I8. Figure S4. <sup>13</sup>C-NMR spectra of compound I8. Figure S5. IR spectra of compound I8.

**Author Contributions:** Formal analysis, S.M.G., H.A.A. (Hoda A. Ahmed), F.S.A. and H.A.A. (Hamud A. Altaleb); Funding acquisition, F.S.A., H.A.A. (Hamud A. Altaleb) and S.M.G.; Methodology, S.M.G., H.A.A. (Hoda A. Ahmed), K.A.A.A.-O. and S.A.P.; Project administration, F.S.A.; Resources, S.A.P. and H.A.A. (Hoda A. Ahmed); Writing—original draft, H.A.A. (Hoda A. Ahmed), S.A.P. and S.M.G.; Writing—review and editing, S.M.G., H.A.A. (Hoda A. Ahmed), F.S.A., H.A.A.

(Hamud A. Altaleb), K.A.A.A.-O. and S.A.P. All authors have read and agreed to the published version of the manuscript.

**Funding:** This research was funded by the Deanship of Scientific Research at Princess Nourah bint Abdulrahman University through the Fast-track Research Funding Program.

**Institutional Review Board Statement:** Not applicable.

**Informed Consent Statement:** Not applicable.

**Data Availability Statement:** Not applicable.

**Acknowledgments:** The authors acknowledge the Deanship of Scientific Research at Princess Nourah bint Abdulrahman University through the Fast-track Research Funding Program.

**Conflicts of Interest:** The authors declare no conflict of interest.

## References

1. Al-Mutabagani, L.; Alshabanah, L.; Gomha, S.; Ahmed, H. Synthesis, Thermal and Optical Characterizations of New Lateral Organic Systems. *Crystals* **2021**, *11*, 551. [[CrossRef](#)]
2. Al-Mutabagani, L.; Alshabanah, L.; Ahmed, H.; Alalawy, H.; Al Alwani, M. Synthesis, Mesomorphic and Computational Characterizations of Nematogenic Schiff Base Derivatives in Pure and Mixed State. *Molecules* **2021**, *26*, 2038. [[CrossRef](#)] [[PubMed](#)]
3. Altowyan, A.; Ahmed, H.; Gomha, S.; Mostafa, A. Optical and Thermal Investigations of New Schiff Base/Ester Systems in Pure and Mixed States. *Polymers* **2021**, *13*, 1687. [[CrossRef](#)] [[PubMed](#)]
4. El-Atawy, M.A.; Naoum, M.M.; Al-Zahrani, S.A.; Ahmed, H.A. New Nitro-Laterally Substituted Azomethine Derivatives; Synthesis, Mesomorphic and Computational Characterizations. *Molecules* **2021**, *26*, 1927. [[CrossRef](#)]
5. Khushaim, M.S.; Alalawy, H.H.; Naoum, M.M.; Ahmed, H.A. Experimental and computational simulations of nematogenic liquid crystals based on cinnamic acid in pure and mixed state. *Liq. Cryst.* **2021**, 1–12. [[CrossRef](#)]
6. Yeap, G.-Y.; Ha, S.; Lim, P.-L.; Boey, P.L.; Ito, M.M.; Sanehisa, S.; Youhei, Y. Synthesis, physical and mesomorphic properties of Schiff base esters containing ortho-, me-ta-, and para-substituents in benzylidene-4'-alkanoyloxyanilines. *Liq. Cryst.* **2006**, *33*, 205–211. [[CrossRef](#)]
7. Ha, S.-T.; Ong, L.-K.; Wong, J.P.-W.; Yeap, G.Y.; Lin, H.-C.; Ong, S.-T.; Koh, T.-M. Mesogenic Schiff's base ether with dimethylamino end group. *Phase Transit.* **2009**, *82*, 387–397. [[CrossRef](#)]
8. Bhatt, H.S.; Patel, P.D.; Dave, J.S. Study of mixed mesomorphism in binary systems of azo-ester mesogens with structurally dis-similar nonmesogenic as well as mesogenic ester homologues. *Mol. Cryst. Liq. Cryst.* **2013**, *587*, 80–91. [[CrossRef](#)]
9. Naoum, M.M.; Fahmi, A.A.; Abaza, A.H.; Saad, G.R. Effect of exchange of terminal substituents on the mesophase behaviour of some azo/ester compounds. *Liq. Cryst.* **2014**, *41*, 1559–1568. [[CrossRef](#)]
10. Alamro, F.S.; Gomha, S.M.; Shaban, M. Optical investigations and photoactive solar energy applications of new synthesized Schiff base liquid crystal derivatives. *Sci. Rep.* **2021**, *11*, 1–11. [[CrossRef](#)]
11. Prajapati, K.; Pandya, H. Azomesogens with 1,2,4-trisubstituted benzene moiety. *Bull. Mater. Sci.* **2002**, *25*, 355–358.
12. Prajapati, K.; Pandya, H. Azomesogens with methoxyethyl tail: Synthesis and characterization. *J. Chem. Sci.* **2005**, *117*, 255–261. [[CrossRef](#)]
13. Alshabanah, L.A.; Al-Mutabagani, L.A.; Gomha, S.M.; Ahmed, H.A.; Popoola, S.A.; Shaban, M. Novel Sulphonic Acid Liquid Crystal Derivatives; Experimental, Computational and Optoelectric Characterizations. *RSC Adv.* **2021**. Accepted RA-ART-03-2021-002517.
14. Saccone, M.; Kuntze, K.; Ahmed, Z.; Siiskonen, A.; Giese, M.; Priimagi, A. ortho-Fluorination of azophenols increases the mesophase stability of photoresponsive hydrogen-bonded liquid crystals. *J. Mater. Chem. C* **2018**, *6*, 9958–9963. [[CrossRef](#)]
15. Jessy, P.; Radha, S.; Patel, N. Morphological, optical and dielectric behavior of chiral nematic liquid crystal mixture: Study on effect of different amount of chirality. *J. Mol. Liq.* **2018**, *255*, 215–223. [[CrossRef](#)]
16. Mishra, R.; Hazarika, J.; Hazarika, A.; Gogoi, B.; Dubey, R.; Bhattacharjee, D.; Singh, K.N.; Alapati, P.R. Dielectric properties of a strongly polar nematic liquid crystal compound doped with gold nanoparticles. *Liq. Cryst.* **2018**, *45*, 1661–1671. [[CrossRef](#)]
17. Zaki, A.A. Optical measurements of phase transitions in difluorophenylazophenyl benzoate thermotropic liquid crystal with specific orientated fluorine atoms. *Phase Transit.* **2018**, *92*, 135–148. [[CrossRef](#)]
18. Naoum, M.M.; Saad, G.R.; Nessim, R.I.; Abdel-Aziz, T.A.; Seliger, H. Effect of molecular structure on the phase behaviour of some liquid crystalline compounds and their binary mixtures II. 4-Hexadecyloxyphenyl arylates and aryl 4-hexadecyloxy benzoates. *Liq. Cryst.* **1997**, *23*, 789–795. [[CrossRef](#)]
19. Saad, G.R.; Nessim, R.I. Effect of molecular structure on the phase behaviour of some liquid crystalline compounds and their binary mixtures VI [1]. The effect of molecular length. *Liq. Cryst.* **1999**, *26*, 629–636. [[CrossRef](#)]
20. Naoum, M.; Mohammady, S.; Ahmed, H. Lateral protrusion and mesophase behaviour in pure and mixed states of model compounds of the type 4-(4'-substituted phenylazo)-2-(or 3)-methyl phenyl-4'-alkoxy benzoates. *Liq. Cryst.* **2010**, *37*, 1245–1257. [[CrossRef](#)]
21. Luckhurst, G.; Gray, G.W. *The Molecular Physics of Liquid Crystals*; Academic Press: Cambridge, MA, USA, 1979.

22. Sarkar, S.D.; Choudhury, B. Study of binary mixtures of two liquid crystalline samples showing induced smectic phase. *Assam Univ. J. Sci. Technol.* **2010**, *5*, 167–168.
23. Ahmed, H.; Naoum, M. Mesophase behavior of binary and ternary mixtures of benzoic acids bearing terminal substituents of different polarity and chain-lengths. *Thermochim. Acta* **2014**, *575*, 122–128. [[CrossRef](#)]
24. Alhaddad, O.A.; Ahmed, H.A.; Hagar, M.; Saad, G.R.; Al-Ola, A.; Khulood, A.; Naoum, M.M. Thermal and Photophysical Studies of Binary Mixtures of Liquid Crystal with Different Geometrical Mesogens. *Crystals* **2020**, *10*, 223. [[CrossRef](#)]
25. Al-Mutabagani, L.A.; Alshabanah, L.A.; Ahmed, H.A.; El-Atawy, M.A. Synthesis, Optical and DFT Characterizations of Laterally Fluorinated Phenyl Cinnamate Liquid Crystal Non-Symmetric System. *Symmetry* **2021**, *13*, 1145. [[CrossRef](#)]
26. Dave, J.S.; Menon, M. Azomesogens with a heterocyclic moiety. *Bull. Mater. Sci.* **2000**, *23*, 237–238. [[CrossRef](#)]
27. Ahmed, H.; Saad, G. Mesophase behaviour of laterally di-fluoro-substituted four-ring compounds. *Liq. Cryst.* **2015**, *42*, 1765–1772. [[CrossRef](#)]
28. Ahmed, H.A.; El-Atawy, M.A. Synthesis, mesomorphic and geometrical approaches of new non-symmetrical system based on central naphthalene moiety. *Liq. Cryst.* **2021**, 1–13. [[CrossRef](#)]
29. El-Atawy, M.A.; Alhaddad, O.A.; Ahmed, H.A. Experimental and geometrical structure characterizations of new synthesized laterally fluorinated nematogenic system. *Liq. Cryst.* **2021**, 1–11. [[CrossRef](#)]
30. Al-Zahrani, S.A.; Ahmed, H.A.; El-Atawy, M.A.; Abu Al-Ola, K.A.; Omar, A.Z. Synthetic, Mesomorphic, and DFT Investigations of New Nematogenic Polar Naphthyl Benzoate Ester Derivatives. *Materials* **2021**, *14*, 2587. [[CrossRef](#)]
31. Gomha, S.M.; Kheder, N.A.; Abdelhamid, A.O.; Mabkhot, Y.N. One Pot Single Step Synthesis and Biological Evaluation of Some Novel Bis(1,3,4-thiadiazole) Derivatives as Potential Cytotoxic Agents. *Molecules* **2016**, *21*, 1532. [[CrossRef](#)]
32. Gomha, S.M.; Muhammad, Z.A.; Abdel-Aziz, H.M.; Matar, I.K.; El-Sayed, A.A. Green synthesis, molecular docking and anticancer activity of novel 1,4-dihydropyridine-3,5-Dicarbohydrazones under grind-stone chemistry. *Green Chem. Lett. Rev.* **2020**, *13*, 6–17. [[CrossRef](#)]
33. Gomha, S.M.; Abdelhady, H.A.; Hassain, D.Z.; Abdelmonsef, A.H.; El-Naggar, M.; Elaasser, M.M.; Mahmoud, H.K. Thiazole-Based Thiosemicarbazones: Synthesis, Cytotoxicity Evaluation and Molecular Docking Study. *Drug Des. Dev. Ther.* **2021**, *15*, 659–677. [[CrossRef](#)] [[PubMed](#)]
34. Sayed, R.; Abd El-lateef, H.M.; Gomha, S.M. L-Proline catalyzed green synthesis and anticancer evaluation of novel bioactive benzil bis-hydrazones under grinding technique. *Green Chem. Lett. Rev.* **2021**, *14*, 179–188. [[CrossRef](#)]
35. Abu-Melha, S.; Edrees, M.M.; Riyadh, S.M.; Abdelaziz, M.R.; Elfiky, A.A.; Gomha, S.M. Clean grinding technique: A facile synthesis and in silico antiviral activity of hydrazones, pyrazoles, and pyrazines bearing thiazole moiety against SARS-CoV-2 main protease (Mpro). *Molecules* **2020**, *25*, 4565. [[CrossRef](#)]
36. Sayed, A.R.; Gomha, S.M.; Taher, E.A.; Muhammad, Z.A.; El-Seedi, H.R.; Gaber, H.M.; Ahmed, M.M. One-Pot Synthesis of Novel Thiazoles as Potential Anti-Cancer Agents. *Drug Des. Dev. Ther.* **2020**, *14*, 1363–1375. [[CrossRef](#)] [[PubMed](#)]
37. Ouf, S.A.; Gomha, S.M.; Eweis, M.; Ouf, A.S.; Sharawy, I.A.A.; Alharbi, S.A. Antidermatophytic activity of some newly synthesized arylhydrazonothiazoles conjugated with monoclonal antibody. *Sci. Rep.* **2020**, *10*, 1–8. [[CrossRef](#)]
38. Gomha, S.M.; Edrees, M.M.; Muhammad, Z.A.; Kheder, N.A.; Abu-Melha, S.; Saad, A.M. Synthesis, Characterization, and Antimicrobial Evaluation of Some New 1,4-Dihydropyridines-1,2,4-Triazole Hybrid Compounds. *Polycycl. Aromat. Compd.* **2020**, 1–13. [[CrossRef](#)]
39. Gomha, S.M.; Riyadh, S.M. Synthesis under Microwave Irradiation of [1,2,4]Triazololo[3,4-b][1,3,4]thiadiazoles and Other Diazoles Bearing Indole Moieties and Their Antimicrobial Evaluation. *Molecules* **2011**, *16*, 8244–8256. [[CrossRef](#)]
40. Rashdan, H.R.M.; Abdelmonsef, A.H.; Shehadi, I.A.; Gomha, S.M.; Soliman, A.M.M.; Mahmoud, H.K. Synthesis, molecular docking screening and anti-proliferative potency evaluation of some new imidazo[2,1-b]thiazole linked thiadiazole conjugates. *Molecules* **2020**, *25*, 4997. [[CrossRef](#)]
41. Frisch, M.J.; Trucks, G.W.; Schlegel, H.B.; Scuseria, G.E.; Robb, M.A.; Cheeseman, J.R.; Scalmani, G.; Barone, V.; Mennucci, B.; Petersson, G.A.; et al. *Gaussian 09, Revision A.02*; Gaussian, Inc.: Wallingford, CT, USA, 2009.
42. Becke, A.D. Density-functional exchange-energy approximation with correct asymptotic behavior. *Phys. Rev. A* **1988**, *38*, 3098–3100. [[CrossRef](#)]
43. Lee, C.; Yang, W.; Parr, R.G. Development of the Colle-Salvetti correlation-energy formula into a functional of the electron density. *Phys. Rev. B* **1988**, *37*, 785–789. [[CrossRef](#)]
44. Al-Mutabagani, L.A.; Alshabanah, L.A.; Naoum, M.M.; Hagar, M.; Ahmed, H.A. Experimental and computational approaches of newly polymorphic supramolecular H-bonded liquid crystal complexes. *Front. Chem.* **2020**, *8*, 571120. [[CrossRef](#)]
45. Hagar, M.; Ahmed, H.; El-Sayed, T.; Alnoman, R. Mesophase behavior and DFT conformational analysis of new symmetrical diester chalcone liquid crystals. *J. Mol. Liq.* **2019**, *285*, 96–105. [[CrossRef](#)]
46. Takase, A.; Nonaka, K.; Koga, T.; Sakagami, S. Raman Spectroscopic Study of Liquid Crystalline N-[4-(4-n-Alkoxybenzoyloxy)-2-Hydroxybenzylidene]-Chloroanilines. *Mol. Cryst. Liq. Cryst. Sci. Technol. Sect. A Mol. Cryst. Liq. Cryst.* **2001**, *357*, 249–262. [[CrossRef](#)]
47. Hagar, M.; Ahmed, H.A.; Saad, G.R. Mesophase stability of new Schiff base ester liquid crystals with different polar substituents. *Liq. Cryst.* **2018**, *45*, 1324–1332. [[CrossRef](#)]

- 
48. Popoola, S.A.; Al-Harbi, M.H.M.; Al-Rashidi, A.H.; Almarwani, M.S.A.; Almohammed, A.R.; Logunleko, A.O.; Al-Saadi, A.A. DFT evaluation of the effects of OH, NH<sub>2</sub> and Br substituents on the properties of 2,2'-bipyridine derivatives. *J. Taibah Univ. Sci.* **2020**, *14*, 1527–1537. [[CrossRef](#)]
  49. Popoola, S.A.; Almohammed, A.R.; Haruna, K. Spectroscopic and DFT evaluation of the positional effect of amino group on the properties of aminobenzenesulphonic acid: Solvents interactions. *Chem. Pap.* **2021**, *75*, 2775–2789. [[CrossRef](#)]